Fluid 'rope trick' investigated

Buckling instabilities can arise from competition between axial compression and bending in slender objects. These are not restricted to solids, but also occur with fluids with free surfaces[1–4], in geophysics[5] and in materials processing[6]. Here we consider a classic demonstration of fluid buckling[7].

When honey is poured from a sufficient height, it approaches one's toast as a thin filament which whirls steadily around the vertical forming a regular helical coil (illustrated with silicone oil in Fig. 1), a behaviour reminiscent of the coiling of a falling flexible rope[8]. We derive a scaling law that predicts the coiling frequency in terms of the filament radius and the flow rate.

The physical parameters governing the phenomenon include the fluid density ρ, viscosity μ (kinematic viscosity $\nu = \mu/\rho$), the flow rate Q, gravity g, a characteristic filament radius r, and the height, h, over which the filament falls. As h is gradually increased, the axial stagnation flow becomes unstable to bending disturbances and the filament is steadily laid out in a circular coil of radius R at a frequency Ω.

The onset of the instability[9–11] is determined by the relative magnitude of the gravitational timescale $(h/g)^{1/2}$ and the viscous timescale $r^2\rho/\mu$, characterized by a slenderness ratio $\epsilon = r/h$, or a Reynolds number $\mathrm{Re} = gr^3/\nu^2$. We note that a similar parameter $\rho g h^3/B$, where B is the bending stiffness, occurs in the elastic analogue[8]. Only below a critical value of ϵ or Re is the axisymmetric stagnation flow unstable. Far from onset, when ϵ becomes sufficiently small, the flow is still mainly an axial stretching flow. However, in a small neighbourhood of the flat surface there is a highly nonlinear coiling region, which persists over a range of falling heights.

In this region, the filament radius is constant (Fig. 1), and the rotatory inertial forces due to the whirling dominate gravity and are balanced by the viscous forces due to the differential velocities between the inner and outer segments of a curved filament. The characteristic radius of curvature of the filament scales with the coil radius R, as for a coiling rope[8]. Then the differential velocity scales as Ur/R, where U is the axial velocity. The Newtonian viscous force per unit volume scales as $\mu Ur/R^3$. The force per unit volume due to centripetal and Coriolis accelerations scales as $\rho\Omega^2 R$. Balancing the two forces yields

$$\mu Ur/R^3 \sim \rho\Omega^2 R \qquad (1).$$

A filament of almost constant diameter is laid out in a steady circular coil near the flat surface $U \sim \Omega R$, whereas continuity of the axial stretching flow yields $Ur^2 \sim Q$. Substituting these relations into equation (1) yields a scaling law for the coiling frequency

$$\Omega \sim Q^{3/2} r^{-7/2} \nu^{-1/2} \qquad (2).$$

To test these predictions, we studied the coiling of silicone oil, flowing at a constant rate out of circular holes in a steel plate at the base of a large reservoir of fluid. We established the dependence between the coiling frequency and filament radius by varying the height of the fall. The coiling frequency was determined by measuring the intensity fluctuations of a refracted laser aimed at the top of the coiling region. A horizontal microscope with a charge-coupled device camera was used to measure the filament radius with an accuracy of 1%. All measurements were made in a parameter regime far from the onset of coiling and also far from the regime when the coiled column itself is unstable and collapses periodically under its own weight. The data are best fitted by a power law $\Omega/Q^{1.5} \sim r^{-3.58\pm16}$ for each flow rate (Fig. 2), and agree well with the theoretically predicted scaling law[2].

Several effects such as surface tension, the relaxation of Poiseuille flow to plug flow in the neighbourhood of the orifice, air drag, non-Newtonian effects and the effect of gravity in the coiling region, have been neglected here, as they are relatively unimportant. They can be accounted for in a quantitative long-wavelength theory similar to that used to describe coiling of falling ropes[8].

L. Mahadevan
Division of Mechanics and Materials, Mechanical Engineering,1-310, Massachusetts Institute of Technology, Cambridge, MA 02139, USA
e-mail: l_m@mit.edu
William S. Ryu, Aravinthan D.T. Samuel
Department of Molecular and Cellular Biology, Harvard University, Cambridge, MA 02138, USA and Rowland Institute of Science, Cambridge, MA 02142, USA

1. Barnes, G. & Woodcock, R. *Am. J. Phys.* **26,** 205–209 (1958).
2. Taylor, G. I. *Proc. 12th Intl Congr. Appl. Mech.* 382–395 (1969).
3. Benjamin, T. B. & Mullins, T. J. *Fluid Mech.* **195,** 523–540 (1988).
4. Matovich, M. A. & Pearson, J. R. A. *Ind. Engrg. Chem. Fund.* **8,** 605–609 (1969).
5. Johnson, A. M. & Fletcher, R. C. *Folding of Viscous Layers* (Columbia University Press, New York, 1994).
6. Rawson, H. *Phys. Tech.* **2,** 91–114 (1974).
7. Taylor, G.I. *Low Reynolds Number Flows* (*Encyclopaedia Britannica* films, 1967).
8. Mahadevan, L. & Keller, J. B. *Proc. R. Soc. Lond. A* **452,** 1679–1694 (1996).
9. Cruickshank, J. O. & Munson, B. R. *J. Fluid Mech.* **113,** 221–239 (1981).
10. Griffiths R. W. & Turner, J. S. *Geophys. J.* **95,** 397–419 (1988).
11. Tchavdarov, B., Yarin, A. L. & Radev, S. *J. Fluid Mech.* **253,** 593–615 (1993).

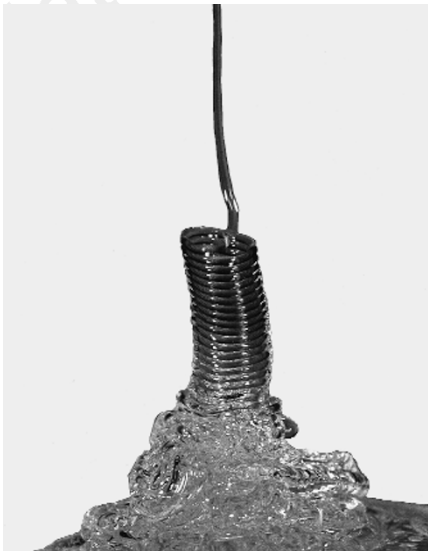

FELICE FRANKEL

Figure 1 Photograph of a coiling filament of silicone oil (PDMS, μ=1.019 × 10^3 g cm^{-1} s, ρ=1 g cm^{-3}; Gelest), highlighting the constant-diameter coils of diameter of approximately 0.5 cm near the surface.

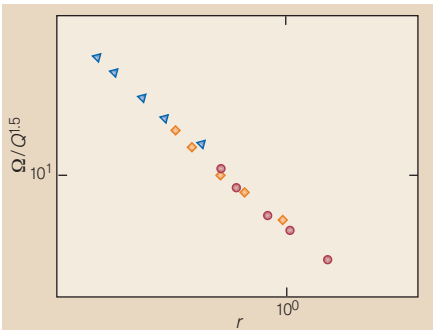

Figure 2 Log–log plot of the normalized coiling frequency (Ω/Q^{15}) against filament radius (r). Triangle: hole radius, 3.2 mm, Q=0.56 g s^{-1}; diamond: hole radius, 4.0 mm, Q =0.96 g s^{-1}; circle: hole radius, 4.8 mm, Q=1.28 g s^{-1}. The data are fitted by the relation $\Omega/Q^{15} \sim r^{3.58\pm16}$ for each flow rate, and confirm equation (2).

Alzheimer's peptide kills cells of retina *in vivo*

Alzheimer's disease, the commonest form of dementia, is a progressive, age-dependent disorder characterized by the presence of large numbers of senile plaques and neurofibrillary tangles[1]. The neuritic plaques consist of an accumulation of amyloid-β peptide (Aβ); this substance, which derives from proteolysis of β-amyloid precursor protein (APP), seems to play a central role in the pathology of the disease. The toxicity of Aβ to neurons has already been demonstrated *in vitro*. Here we show that the peptide is also cytotoxic *in vivo*.

Support for the role of Aβ in Alzheimer's comes from reports showing that mutations in the gene encoding APP, and in other genes involved in the disease, lead to overproduction of the more amyloidogenic 42 amino-acid residue long isoform of Aβ, $A\beta_{1-42}$. Transgenic mice overexpressing the gene for APP show similar changes, and aggregated Aβ is toxic to cultured neurons of the cerebral cortex or

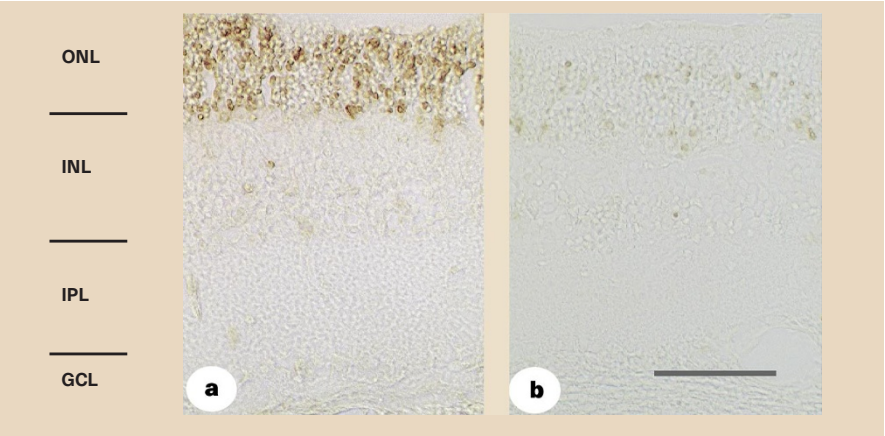

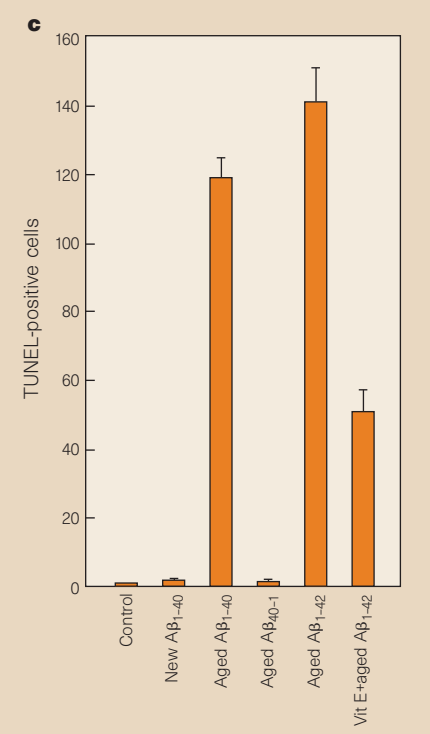

Figure 1 Representative photomicrographs showing TUNEL staining in retinal sections from eyes of rats given unilateral intravitreal injection of **a,** aged $A\beta_{1-42}$ (2 nmol in 3 μl); or **b,** vitamin E (1.3 μg in 3μl) plus aged $A\beta_{1-42}$ (2 nmol in 3 μl) 30 min later. After two days, rats were perfused with fixative and retinas were processed for TUNEL staining. **c,** Number of TUNEL-positive cells (mean of ten 390-μm-long sections) in the outer nuclear layer (ONL) of 2–4 retinas injected with control (3 μl vehicle), new $A\beta_{1-40}$ (2 nmol in 3 μl), aged $A\beta_{1-40}$ (2 nmol in 3 μl), aged $A\beta_{40-1}$ (2 nmol in 3 μl) and the two groups mentioned above. Vitamin E pretreatment produced a significant reduction in the number of TUNEL-positive ONL cells. The purity of the Aβ peptides was confirmed by sequencing and mass spectrometry (Bachem). INL, inner nuclear layer; IPL, inner plexiform layer; GCL, ganglion cell layer. Bar, 50 μm.

the hippocampus *in vitro*[1–3]. Although the mechanisms by which Aβ causes neuronal death are not fully understood, *in vitro* results suggest that an increase in oxidative stress and destabilization of calcium homeostasis[2,3] are involved.

However, in contrast to these *in vitro* observations[2–4], only a slight neurotoxicity results when Aβ is directly administered to the brain[5,6], perhaps because of the rapid efflux of injected compounds from this organ.

In this respect another organ, the retina, offers several advantages. It is an integral part of the central nervous system; its structure is well organized; and, because it is a closed system, injected compounds remain in the vitreous body for a long time[7].

We investigated the cytotoxic effects of Aβ on retinal cells after intravitreal injection and the amelioration of these effects by the antioxidant vitamin E. The technique used to assess apoptosis and therefore cytotoxicity was terminal deoxynucleotidyl transferase dUTP-end-labelling (TUNEL) staining. This technique identifies the 3′ ends of DNA strands — a phenomenon resulting from the fragmentation of DNA that occurs in apoptotic cells.

When the retinas of rats were injected with either aged $A\beta_{1-42}$ or aged $A\beta_{1-40}$ (aggregated; incubated for 4 days at 37 °C), a distinct band of TUNEL-positive photoreceptor cells was evident in the retina's outer nuclear layer. However, in the inner nuclear layer and ganglion cell layer, only a few scattered cells were TUNEL positive (Fig. 1a). This suggests that proximity to the Aβ injection site is not essential for cytotoxicity.

In addition, all retinas injected with the freshly prepared, 'new' $A\beta_{1-40}$ behaved like vehicle-injected and uninjected retinas in showing only occasional TUNEL-positive cells (Fig. 1c). Therefore the cytotoxic effect was specific to treatment with aggregated Aβ. Moreover, unlike active aged $A\beta_{1-40}$, inactive aged reverse $A\beta_{40-1}$ did not induce any changes in photoreceptor cells (Fig. 1c). No DNA fragmentation was seen in the glial cells. But, as with cultured neural cells *in vitro*[8], treatment with $A\beta_{1-42}$ or $A\beta_{1-40}$ severely decreased Bcl-2 immunoreactivity in the endfeet and proximal part of radial processes of Müller glial cells.

In vitro studies also suggested that Aβ causes an accumulation of hydrogen peroxide and lipid peroxides in the cells, and that antioxidants protect cells from Aβ toxicity[2,3]. We found that TUNEL-positive photoreceptor cells in retinas that had been pretreated with vitamin E (1.3 micrograms per 3 microlitres) showed a reduction of about 65% compared with retinas treated with aged $A\beta_{1-42}$ (Fig. 1). This indicates that Aβ cytotoxicity is caused, at least partly, by a free-radical mechanism.

Doubts have been raised in the past about extrapolating *in vitro* findings on Aβ cytotoxicity to the situation *in vivo*. Our results show that some of the proposed mechanisms underlying Aβ neurotoxicity do operate *in vivo*. In addition, the closed 'retina–vitreal' system we describe should serve as an experimental model for further *in vivo* studies and for testing appropriate compounds for their ameliorating effects on Aβ-mediated neurotoxicity.

L. S. Jen, A. J. Hart*, A. Jen, J. B. Relvas, S. M. Gentleman, L. J. Garey, A. J. Patel
MRC Laboratory and Department of Neurodegenerative Disorders, Division of Neuroscience, Imperial College School of Medicine, Charing Cross Hospital, Fulham Palace Road, London W6 8RF, UK
e-mail: a.patel@cxwms.ac.uk
** Present address: The National Hospital for Neurology and Neurosurgery, Queen Square, London, WC1N 3BG, UK*

1. Selkoe, D .J. *Annu. Rev. Neurosci.* **17,** 489–517 (1994).
2. Mark, R. J., Blanc, E. M. & Mattson, M. P. *Mol. Neurobiol.* **12,** 211–224 (1996).
3. Cotman, C. W. & Su, J. H. *Brain Pathol.* **6,** 493–506 (1996).
4. Gray, C. W. & Patel, A. *J. Brain Res.* **691,** 169–179 (1995).
5. Games, D. *et al. Neurobiol. Aging* **13,** 569–576 (1992).
6. Podlinsky, M. B. *et al. Am. J. Pathol.* **142,** 17–24 (1993).
7. Mey, J. & Thanos, S. *Brain Res.* **602,** 304–317 (1993).
8. Paradis, E., Douillard, H., Koutroumanis, M., Goodyer, C. & LeBlanc A. *J. Neurosci.* **16,** 7533–7539 (1996).

Are retrotransposons long-term hitchhikers?

Transposable elements represent a large fraction of the genomes of eukaryotes, and yet we know little of their origins or stability. Striking examples of cross-species transfer have been discovered among *mariner* elements[1] (transposable elements that are widespread in insects and other animals), confirming the impression that horizontal transfers are essential to the long-term success of transposable elements. We show that R1 and R2, two distantly related non-long-